Observation of non-Hermitian aggregation effects induced by strong interactions

Weixuan Zhang,[1] Fengxiao Di,[1] Hao Yuan ◉,[1] Haiteng Wang,[1] Xingen Zheng,[1] Lu He ◉,[1]
Houjun Sun ◉,[2] and Xiangdong Zhang ◉[1,*]

[1]*Key Laboratory of Advanced Optoelectronic Quantum Architecture and Measurements of Ministry of Education,*
Beijing Key Laboratory of Nanophotonics & Ultrafine Optoelectronic Systems, School of Physics,
Beijing Institute of Technology, 100081 Beijing, China
[2]*Beijing Key Laboratory of Millimeter Wave and Terahertz Techniques, School of Information and Electronics,*
Beijing Institute of Technology, 100081 Beijing, China

Non-Hermiticity greatly expands existing physical laws beyond the Hermitian framework, revealing various phenomena with unique properties. To date, most exotic non-Hermitian effects, such as exceptional points and non-Hermitian skin effects, have been discovered in single-particle systems. The interplay between non-Hermitian and particle interactions is expected to be a more fascinating but much less explored area. Here, we report an experimental simulation of a strongly correlated non-Hermitian few-body system and reveal a type of non-Hermitian skin state toward effective boundaries in Hilbert space induced by strong interactions. Such an interaction-induced non-Hermitian effect represents the aggregation of bosonic clusters with nonidentical occupations in the periodic lattice, and we call it the non-Hermitian aggregation effect. By mapping the eigenstates of three correlated bosons to modes of the designed three-dimensional electric circuit, the interaction-induced non-Hermitian aggregation effects in Hilbert space are verified by measuring the spatial impedance response. Our finding not only discloses a physical effect in the non-Hermitian system but also suggests a flexible platform to further investigate other non-Hermitian correlated phases in experiments.

I. INTRODUCTION

Exploring physical phenomena in strongly correlated quantum systems is one of the most difficult challenges in modern physics, where particle interactions could play key roles in the formation of various correlated quantum phases [1–5]. Especially from an experimental perspective, early efforts on interaction quantum physics have mainly focused on the Hermitian system. Recent developments in non-Hermitian physics have opened exciting opportunities to exhibit exotic behaviors beyond the Hermitian framework [6–30]. One representative example is the non-Hermitian skin effect [14–19], where the energy eigenvalues and corresponding eigenstates are changed in a nonlocal way with distant boundary conditions. Following the discovery of non-Bloch eigenstates related to non-Hermitian skin effects, various intriguing phenomena, such as the modified bulk-boundary correspondence [14–23] and non-Hermitian critical behavior [24], have been proposed. Subsequently, the experimental observation of non-Hermitian skin effects has been realized in a variety of nonconservative systems [25–28], providing versatile platforms for exploring unconventional wave phenomena and giving rise to many applications in the field of the non-Hermitian sensor [29] and topological wave funneling [30].

Compared with the single-particle system, the interaction non-Hermitian system may show more exotic features. Motivated by the development of non-Hermitian single-particle physics, there have been emerging theoretical interests in de-

veloping phenomena originating from the interplay between non-Hermitian and particle correlations [31–39]. It has been pointed out in a recent work that many-body skin states could locate toward effective boundaries in Hilbert space for the periodic lattice [40]. Those effective boundaries are induced by the species-dependent asymmetric hopping for the periodic many-body system, while it is still unclear what skin-like effects could appear in the non-Hermitian system with strong interactions. In addition, despite their central importance, it remains challenging to simulate these correlated non-Hermitian phases in experiments [41], even for few-body cases. In this case, a newly accessible and fully controllable platform is expected to simulate correlated non-Hermitian systems.

In this paper, we demonstrate that strong interaction can create effective boundaries in Hilbert space and induces a type of non-Hermitian skin state. Based on the analytical derivations and numerical simulations, it is found that these interaction-induced non-Hermitian skin states represent the aggregation of bosonic clusters with nonidentical occupations in the periodic lattice. In experiments, using a three-boson system as an illustration, we map the corresponding eigenstates to modes of the designed circuit lattice, and the non-Hermitian few-body aggregation effect is verified by measuring the spatial impedance response.

II. INTERACTION-INDUCED NON-HERMITIAN AGGREGATION EFFECTS

We consider correlated bosons with asymmetric hoppings on a one-dimensional (1D) chain under the periodic boundary condition (PBC). The lattice length is L, and the number of
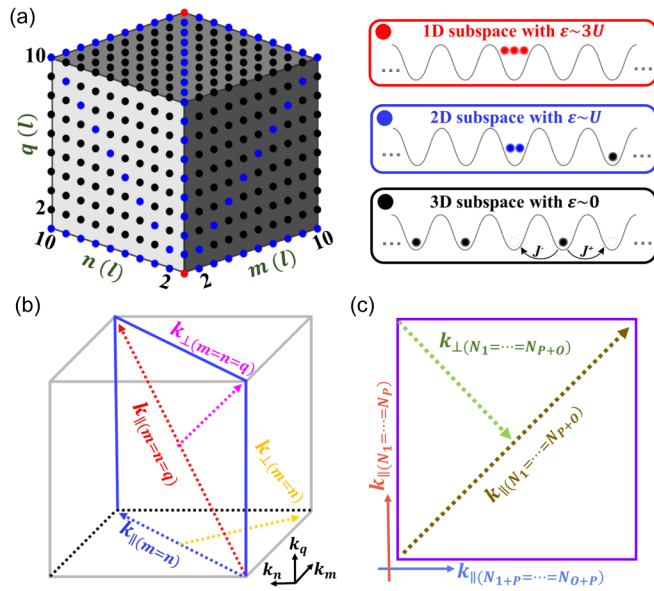
*zhangxd@bit.edu.cn

FIG. 1. Interaction-induced non-Hermitian aggregation effects in Hilbert space. (a). The three-dimensional (3D) configuration space for the probability amplitude of three bosons. (b). Illustration of wave vectors parallel/perpendicular to both one-dimensional (1D) and two-dimensional (2D) effective boundaries. (c). Schematic diagram of wave vectors parallel/perpendicular to the effective boundary in the N-boson subspace with two bosonic clusters.

bosons is N. The system can be described by the nonreciprocal 1D Bose-Hubbard Hamiltonian as

$$H = -\sum_l [J^+ a_{l+1}^+ a_l + J^- a_l^+ a_{l+1}] + 0.5U \sum_l n_l(n_l - 1),$$
(1)

where a_l^+ (a_l) and $n_l = a_l^+ a_l$ are the creation (annihilation) and particle number operators, respectively. Here, $J^\pm$ define asymmetric hopping strengths along positive and negative directions, and U corresponds to the onsite interaction energy. We start to consider a simple case with $N = 3$. The three-boson solution can be expanded in Hilbert space as $|\psi\rangle = \frac{1}{\sqrt{6}} \sum_{m,n,q=1}^L c_{mnq} a_m^+ a_n^+ a_q^+ |0\rangle$, where $|0\rangle$ is the vacuum state, and c_{mnq} is the probability amplitude of the first, second, and third bosons at sites m, n, and q. Substituting the Hamiltonian and $|\psi\rangle$ into the stationary Schrödinger equation $H|\psi\rangle = \varepsilon |\psi\rangle$, we obtain the eigenequation with respect to c_{mnq} as

$$\varepsilon c_{mnq} = -J^+ (c_{m+1,n,q} + c_{m,n+1,q} + c_{m,n,q+1})$$
$$- J^- (c_{m-1,n,q} + c_{m,n-1,q} + c_{m,n,q-1})$$
$$+ U(\delta_{mn} + \delta_{mq} + \delta_{nq}) c_{mnq}.$$
(2)

To illustrate the distribution of probability amplitude for three bosons at different energy scales, we divide the configuration space of c_{mnq} into three subspaces, as shown in Fig. 1(a). Without loss of generality, the lattice length is set as $L = 10$. Red dots on the diagonal line of the configuration space ($m = n = q$) correspond to the subspace with three bosons located at the same lattice site, where the eigenenergy and dimension are $\varepsilon \sim 3U$ and 1D, respectively, as illustrated by the inset enclosed with a red frame. Blue dots on

the diagonal plane ($m = n \neq q$, $m = q \neq n$, and $n = q \neq m$) represent the subspace with two bosons locating at the same lattice site, as shown in the inset with a blue frame, where the effective energy is $\varepsilon \sim U$ and the dimension is two-dimensional (2D). Black dots correspond to the subspace with three bosons located at different lattice sites, as presented in the inset with a black frame, and the corresponding energy scale and configuration dimensions are $\varepsilon \sim 0$ and three-dimensional (3D), respectively. When the onsite interaction is extremely strong ($U \gg J^\pm$), the energy mismatch between these three subspaces becomes very large, making the higher-energy subspace perform like a potential barrier embedding in the lower-energy subspace with higher dimensionality [42–45]. In this case, the 2D (1D) subspace with energy being $\varepsilon \sim U$ ($\varepsilon \sim 3U$) can be regarded as the effective boundary for the 3D (2D) subspace with $\varepsilon \sim 0$ ($\varepsilon \sim U$).

To clarify the distribution of probability amplitude toward these effective boundaries, hopping strengths perpendicular to these boundaries should be analyzed. As shown in Fig. 1(b), we plot wave vectors parallel/perpendicular to the effective 2D (and 1D) boundary in the 3D (and 2D) subspace. Here, $\mathbf{k}_m$, $\mathbf{k}_n$, and $\mathbf{k}_q$ represent wave vectors of three bosons in the periodic lattice. In this case, wave vectors parallel and perpendicular to the effective 2D boundary ($m = n \neq q$) in the 3D subspace can be expressed as $\mathbf{k}_{\|(m=n),\perp(m=n)} = \mathbf{k}_m \pm \mathbf{k}_n$. Moreover, $\mathbf{k}_{\|(m=n=q)}$ and $\mathbf{k}_{\perp(m=n=q)}$, which are in the form of $\mathbf{k}_{\|(m=n=q),\perp(m=n=q)} = \mathbf{k}_{\|(m=n)} \pm \mathbf{k}_q$, correspond to wave vectors parallel and perpendicular to the effective 1D boundary ($m = n = q$) in the 2D subspace.

Using these predefined wave vectors, we first formulate hopping amplitudes in the 3D subspace perpendicular to 2D effective boundaries. For this purpose, the three-boson Bloch Hamiltonian is expressed in the form of a Hatano-Nelson chain [46] in the direction perpendicular to the 2D boundary ($m = n \neq q$) as

$$H(k_{\perp(m=n)}) = J_m^\pm \exp(\pm ik_m) + J_n^\pm \exp(\pm ik_n)\exp[\pm ik_{\perp(m=n)}].$$
(3)

Here, the $\pm$ notation represents two terms written in a combined form. For instance, the term $J_n^\pm \exp(\pm ik_n)$ corresponds to two added terms as $J_n^+ \exp(+ik_n) + J_n^- \exp(-ik_n)$. Here, $J_i^\pm$ are the asymmetric hoppings along the direction of $\pm \mathbf{k}_i$ with $i = m$ or n. Also, $J_{\perp(m=n)}^\pm = J_m^\pm \exp[\pm ik_{\|(m=n)}]\exp[\mp ik_{\|(m=n)}]$ corresponds to the effective hopping in the direction of $\pm \mathbf{k}_{\perp(m=n)}$. If the effective hopping strengths are unbalanced, the boundary-induced localization of probability amplitudes could appear that is like nonreciprocal single-particle systems with open boundaries. Following direct analytical derivations (see Appendix A for details), the requirement for symmetric hopping amplitudes $|J_{\perp(m=n)}^+| = |J_{\perp(m=n)}^-|$ can be expressed as $(J_m^+)^2 + (J_n^-)^2 = (J_m^-)^2 + (J_n^+)^2$ and $J_m^+ J_n^- = J_m^- J_n^+$. Ensured by the identical principle of bosons, this requirement always holds; that is, the balanced hopping strengths along $\pm \mathbf{k}_{\perp(m=n)}$ are satisfied. Hence, the probability amplitude in the 3D subspace is in the form of extended states perpendicular to the 2D effective boundary.

Then we focus on the 2D subspace sustaining the 1D effective boundary. In this case, we derivate the three-boson Bloch Hamiltonian perpendicular to the 1D effective boundary

($m = n = q$) in the 2D subspace (with $m = n \neq q$) as

$$H\big(k_{\perp(m=n=q)}\big) = J^{\pm}_{\|(m=n)}\exp\big[\pm ik_{\|(m=n)}\big] + J^{\pm}_q\exp(\pm ik_q)$$

$$= J^{\pm}_{\perp(m=n=q)}\exp\big[\pm ik_{\perp(m=n=q)}\big], \qquad (4)$$

where $J^{\pm}_{\perp(m=n=q)} = J^{\pm}_{\|(m=n)}\exp[\pm ik_{\|(m=n=q)}] + J^{\mp}_q\exp[\mp ik_{\|(m=n=q)}]$ are effective hopping strengths along $\pm\mathbf{k}_{\perp(m=n=q)}$. It is noted that the symmetric hopping amplitudes along $\pm\mathbf{k}_{\perp(m=n=q)}$ require the following equations to be satisfied (see Appendix A): $\sum_{i=m,n}(J^+_i)^2 + (J^-_q)^2 = \sum_{i=m,n}(J^-_i)^2 + (J^+_q)^2$, $J^+_m J^+_n = J^-_m J^-_n$, and $J^+_{m,n}J^+_q = J^+_{m,n}J^-_q$. With the identical principle of bosons, we always have $|J^+_{\perp(m=n=q)}| \neq |J^-_{\perp(m=n=q)}|$ in the 2D subspace. In this case, the asymmetric hopping strength perpendicular to the effective 1D boundary could make the probability amplitudes of the three bosons concentrate on this boundary. This phenomenon is like the non-Hermitian skin effect in single-particle systems with open boundaries. However, the strong interaction-induced non-Hermitian skin state in Hilbert space represents the aggravation of two bound bosons (doublon) and an isolated boson in the periodic lattice. Hence, we call this phenomenon the non-Hermitian aggregation effect.

In the following, we generalize non-Hermitian aggregation effects to N-boson systems. The subspace possessing two bosonic clusters is considered, where P bosons (labeled from N_1 to N_P) are located at one lattice site and O bosons (labeled from N_{1+P} to N_{O+P}) are located at another lattice site with $(P, O) \propto \{1, \ldots, N\}$. In this case, the corresponding effective boundary could be the subspace with $(P + O)$ bosons located at the same lattice site and the remaining bosons stay on the original sites. Like the three-boson case, wave vectors parallel/perpendicular to such an effective boundary in an N-boson subspace are illustrated in Fig. 1(c). Here, $\mathbf{k}_{\|(N_1=\cdots=N_P)}$ and $\mathbf{k}_{\|(N_{1+P}=\cdots=N_{O+P})}$ represent center-of-mass wave vectors of bosonic clusters possessing P and O bosons, respectively. In this case, wave vectors parallel and perpendicular to the effective boundary can be expressed as $\mathbf{k}_{\|(N_1=\cdots=N_{O+P}),\,\perp(N_1=\cdots=N_{O+P})} = \mathbf{k}_{\|(N_1=\cdots=N_P)} \pm \mathbf{k}_{\|(N_{1+P}=\cdots=N_{O+P})}$.

In this N-boson subspace, the Bloch Hamiltonian perpendicular to the effective boundary is expressed as

$$H\big[k_{\perp(N_1=\cdots=N_{O+P})}\big] = J^{\pm}_{\perp(N_1=\cdots=N_{O+P})}\exp\big[\pm ik_{\perp(N_1=\cdots=N_{O+P})}\big],$$
$$(5)$$

where $J^{\pm}_{\perp(N_1=\cdots=N_{O+P})} = J^{\pm}_{\|(N_1=\cdots=N_P)}\exp[\pm ik_{\|(N_1=\cdots=N_P)}] + J^{\mp}_{\|(N_{1+P}=\cdots=N_{O+P})}\exp[\mp ik_{\|(N_1=\cdots=N_{O+P})}]$ are the effective hopping strengths along $\pm\mathbf{k}_{\perp(N_1=\cdots=N_{O+P})}$. Following detailed derivations (see Appendix B for details), we find that the asymmetric hopping strength $|J^+_{\perp(N_1=\cdots=N_{O+P})}| \neq |J^-_{\perp(N_1=\cdots=N_{O+P})}|$ along the direction of $\pm\mathbf{k}_{\perp(N_{1+P}=\cdots=N_{O+P})}$ can only exist when the particle numbers of two bosonic clusters are different ($P \neq O$). In this case, the interaction-induced skin state could appear in the subspace sustaining nonidentical occupations. If the PBC is used for the lattice, the system can be described by the Bloch Hamiltonian, which could be used to derive the effective hopping strength perpendicular to the wall in Hilbert space, regardless of the length for the 1D lattice and the value of P and O. In this case, the aggregation of two bosonic clusters with different amounts of bosons should also exist in the non-Hermitian many-body system with different densities.

Meanwhile, whether the ground state could exhibit the non-Hermitian aggregation effect depends on the density of the many-body system. When the density is <1, no more than one boson locates at a single lattice site for the ground state in the strong interaction limit. In this case, the aggregation of two isolated bosons cannot appear for the ground state. Moreover, if the density equals an integer (n), the identical occupation of n bosons should exist for the ground state in the strong interaction limit. Also, the aggregation of bosonic clusters with identical occupations cannot appear for the ground state. Meanwhile, if the density is >1 and not equal to integers, the bosonic clusters with unbalanced occupation numbers should exist in the ground state for the strong interaction limit. Hence, the non-Hermitian aggregation effect should exist in the ground state of many-body systems when the density is >1 and not equal to integers. In addition, it is worth noting that the above-proposed skin states in Hilbert space only appear with PBCs (see Appendix C for numerical results with open boundary conditions).

To demonstrate the predicted non-Hermitian aggregation effect induced by strong interactions, we calculate complex energy spectra and profiles of density of state for the 1D three-boson system. The parameters are set as $J^+ = -1$, $J^- = 0$, $U = 50$, and $L = 10$. Figures 2(a)–2(c) present the complex energy spectra for the three subspaces proposed above. To quantify the localization degree of associated eigenstates, we calculate the participation ratio (PR) PR $= \sum_{i=[1,\,n_d]}|\varphi_i|^{-4}/n_d$, with n_d being the number of eigenstates in the d-dimensional subspace. It is noted that PR is relatively large for extended states, while it approaches zero for localized states. In this case, we can see that only the eigenstates in the 2D subspace exhibit significant localizations.

Then we calculate the normalized density of states in each subspace $\psi_d(m, n, q) = \sum_{i=[1,\,n_d]}|\varphi_i(m, n, q)|^2/M$, as plotted in Figs. 2(d)–2(f). The denominator M corresponds to the maximum value for the sum of all eigenstates in the d-dimensional subspace $M = \sum_{i=[1,\,n_d]}|\varphi_i(m_{\max}, n_{\max}, q_{\max})|^2$. It is clearly shown that the density of states in 3D and 1D subspaces are both in the form of extended states. Only the density of states in the 2D subspace is strongly localized around the 1D effective boundary. These results clearly indicate that the interaction-induced skin effect in the Hilbert space of the three bosons could only appear in the 2D subspace toward the 1D effective boundary. Moreover, we also numerically prove that the localization strength of three-body skin states also depends on the interaction strength and lattice size (see Appendix C). It is found that the localization strength of skin states saturates with increasing the interaction strength or lattice size. Except for the three-boson system, both analytical and numerical results for the four- and five-body cases are also provided in Appendix D. We can see that the non-Hermitian aggregation also appears in these few-body systems.

III. SIMULATING THE INTERACTION-INDUCED NON-HERMITIAN ADDREGATION EFFECTS BY CIRCUIT NETWORKS

The direct observation of interaction-induced non-Hermitian aggregation effect requires the control of nonreciprocal hopping and interaction strengths, which
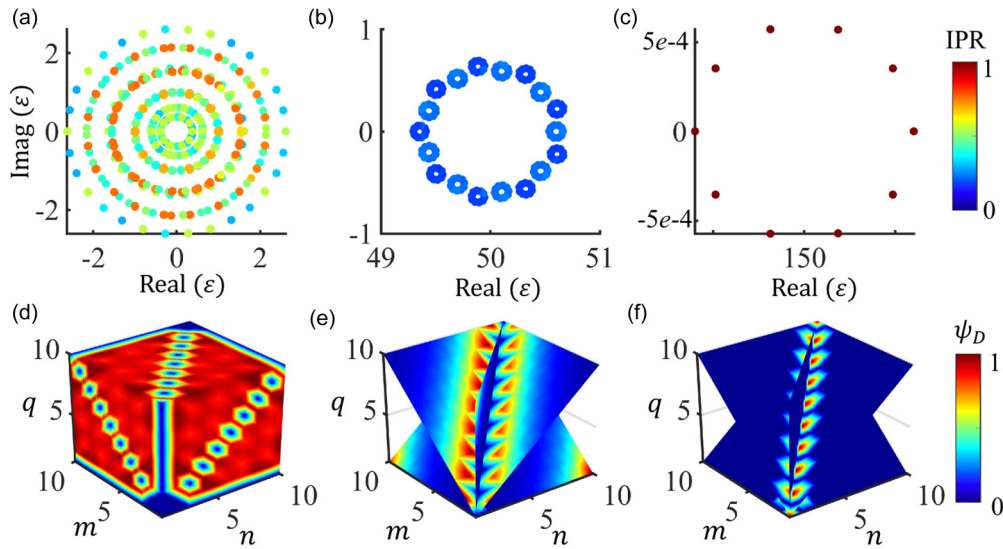
FIG. 2. Results of interaction-induced non-Hermitian aggregation effects for three bosons. (a)–(c) Results of the complex energy spectra of the three-boson system in three subspaces. The color close to blue (red) corresponds to the localized (extended) eigenstates quantified by the participation ratio (PR). (d)–(f) Illustrations of the profiles of normalized density of states in three subspaces.

are hard to realize in quantum systems. In this part, we propose an analog method to construct a circuit lattice to simulate three-body skin states in Hilbert space. It is known that the few-body configuration space can be mapped to the high-dimensional lattice [42–45]. In this case, the configuration state of the three bosons in Fig. 1(a) can be regarded as the 3D lattice modes in the single-particle region. With such an analogy, the probability amplitude of the 1D three-boson model c_{mnq} is directly mapped to that of the single particle located at the lattice site (m, n, q) in 3D space. The nonreciprocal hopping along a certain direction of the mapped 3D lattice represents the asymmetric hopping of one boson in the 1D lattice. The onsite potential at three diagonal planes ($m = n$, $m = q$, and $n = q$) of the mapped 3D lattice can mimic the onsite interaction. In this case, the behavior of the three correlated bosons in the 1D lattice can be effectively simulated by a single particle in the mapped 3D lattice.

Based on the similarity between the circuit Laplacian and the lattice Hamiltonian [47–59], the mapped 3D lattice can be realized by electric circuits. As displayed in Fig. 3(a), we select two planes (m, n, $q = 7$, the green frame, and $m = n$, q, the blue frame) to illustrate the design. Figures 3(b) and 3(c) present the circuit structure at these two planes. The black, blue, and red nodes correspond to three-boson states in 3D, 2D, and 1D subspaces. To fulfill the nonreciprocal coupling of adjacent circuit nodes, the capacitor C_1 is parallelly connected with a one-way coupling capacitor, which is realized by a capacitor C_2 in series with a negative impedance converter with current inversion (INIC) [as shown in Fig. 3(d)]. The particle interaction can be simulated with suitable groundings, where the capacitor C_U ($3C_U$) is selected for extra grounding on the diagonal planes (line) of blue (red) nodes, as presented in Fig. 3(d). The inductor (L_g) is used to link each node to the ground. Moreover, circuit nodes at boundaries are connected end-to-end to realize the PBC. In this case, the circuit eigenequation possesses the same form as the stationary Schrödinger equation of the three bosons (see

Appendix E), where the voltage V_{mnq} at circuit node (m, n, q) corresponds to the three-boson probability amplitude c_{mnq}. The eigenenergy of the three bosons is directly related to the eigenfrequency of the designed circuit as $\varepsilon = f_0^2/f^2 - 6$ with $f_0 = 1/2\pi\sqrt{C_1 L_g}$. Other parameters are $J^\pm = (C_1 \pm C_2)/C_1$ and $U = C_U/C_1$.

To experimentally observe the three-body skin effects, we fabricate the designed 3D circuit, as shown in Fig. 3(e). Ten printed circuit boards (PCBs) are applied with a single PCB containing 10×10 nodes in the mn plane. Enlarged views of the front and back sides of a single PCB are shown in the right insets. We can see that adjacent circuit nodes are connected through the capacitor C_1 (the black circle) and a parallelly connected one-way capacitor, which is consistent with a capacitor C_2 (the red circle) and a negative INIC (the blue block). The grounding capacitor C_U on the diagonal plane is marked by the green block, and the grounding inductor L_g is enclosed by the yellow block. Here, the values of C_1, C_2, C_U, and L_g are taken as 1 nF, 1 nF, 10 nF, and 3.3 μH. Figures 3(f)–3(h) present measured impedances of three nodes along the direction of $\mathbf{k}_{\perp(m=n,q=1)}$ in the 3D subspace, where the selected circuit nodes are labeled by (8,3,1), (7,4,1), and (6,5,1) in Fig. 3(a). We note that impedance peaks of three circuit nodes all appear from 0.8 to 1.5 MHz, matching the corresponding eigenenergy ($\varepsilon \sim 0$) of three bosons in the 3D subspace. It is shown that peak values of these circuit nodes are nearly identical. This indicates that no non-Hermitian aggregation effect appears in the 3D subspace toward the 2D effective boundary. Moreover, in Figs. 3(j)–3(k), we plot measured impedances of three circuit nodes along the direction of $\mathbf{k}_{\perp(m=n=q)}$ in the 2D subspace [(8,8,3), (7,7,4), and (6,6,5) marked by blue dots]. It is shown that significant impedance peaks only exist from 0.6 to 0.8 MHz, and the peak value increases as circuit nodes approach the 1D effective boundary, which is in accordance with the theoretical prediction in Fig. 2(e). Figure 3(l) displays the measured impedance of a circuit node at (4,4,4) in the 1D subspace. It is shown that
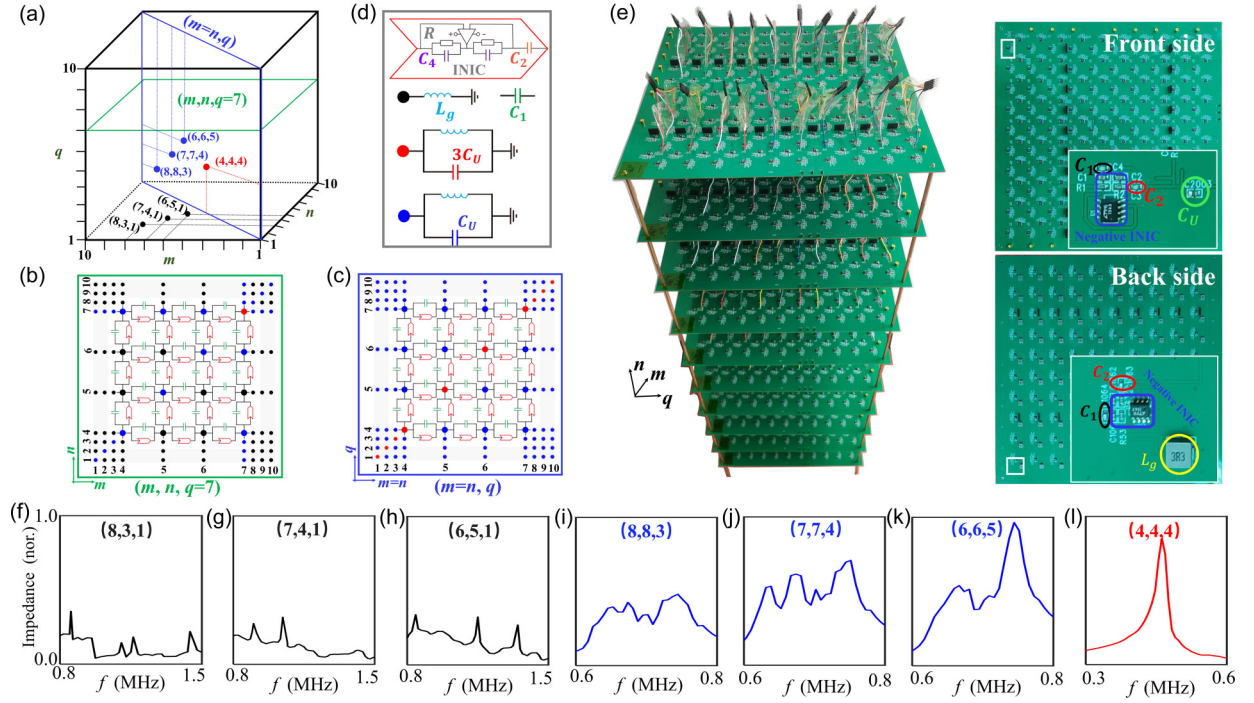
FIG. 3. Experimental simulations of three-body non-Hermitian aggregation effects by circuits. (a) The scheme of two planes $(m, n, q = 7)$ and $(m = n, q)$ in the three-dimensional (3D) circuit. (b) and (c) present the circuit structures of these two planes. (d) The ground setting of different circuit nodes and the structure of the one-way coupling capacitor. (e) Photograph image of the fabricated circuit. Insets plot enlarged views of front and back sides of a single printed circuit board (PCB). The measured impedances of circuit nodes along $k_{\perp(m=n,q=1)}$ in the 3D subspace for (f)–(h), along $k_{\perp(m=n=q)}$ in the two-dimensional (2D) subspace for (i)–(k), and in the one-dimensional (1D) subspace at (4,4,4) for (l).

the peak value appears ~ 0.46 MHz, which is consistent with eigenenergies of $3U$. All experimental results are in accordance with circuit simulations (see Appendix F). The wider peaks than that of the numerical results are mainly due to the larger lossy effect. Approximate results clearly prove the appearance of interaction-induced non-Hermitian aggregation effects in the 2D subspace toward the 1D effective boundary.

IV. CONCLUSIONS

In conclusion, we have demonstrated that strong interaction can induce non-Hermitian aggregation effects in periodic lattices. Direct analytical derivations indicate that the non-Hermitian aggregation effect should appear in subspaces sustaining clusters with different amounts of bosons. In experiments, we map three-boson states to modes of the 3D circuit to simulate the interaction-induced skin states in Hilbert space. It is also interesting to investigate other properties of few-body non-Hermitian aggregation effects based on the designed circuit simulator, such as critical phenomena and competition with disorder-induced localizations. Our proposal provides a flexible platform to investigate and visualize interesting phenomena related to particle interactions and non-Hermitian physics.

Note added. We became aware of a theoretical work [60] that is focused on the skin cluster in non-Hermitian systems.

APPENDIX A: ANALYTICAL DERIVATION OF REQUIREMENTS FOR NON-HERMITIAN AGGREGATION EFFECTS OF THREE BOSONS

In this appendix, we provide a detailed derivation of the requirement of interaction-induced skin states in three-boson subspaces with different dimensions. First, we explore the 3D subspace with three bosons located at different lattice sites, and the associated effective boundaries correspond to the state with only two bosons occupying the same lattice site. In this case, we express the three-boson Bloch Hamiltonian (with $m \neq n \neq q$) in the form of a single-particle Hatano-Nelson chain perpendicular to the 2D boundary $(m = n \neq q)$ as

$$H\big(k_{\perp(m=n)}\big) = J_m^{\pm} \exp(\pm ik_m) + J_n^{\pm} \exp(\pm ik_n)$$
$$= J_{\perp(m=n)}^{\pm} \exp\big[\pm ik_{\perp(m=n)}\big], \qquad (A1)$$

where $J_{\perp(m=n)}^{\pm} = J_m^{\pm} \exp[\pm ik_{\parallel(m=n)}] + J_n^{\mp} \exp[\mp ik_{\parallel(m=n)}]$ are the effective hopping along $\pm k_{\perp(m=n)}$ with $\mathbf{k}_{m,n} = \mathbf{k}_{\parallel(m=n)} \pm \mathbf{k}_{\perp(m=n)}$. If $|J_{\perp(m=n)}^+| \neq |J_{\perp(m=n)}^-|$, skin states could exist toward

this effective 2D boundary. To judge the relationship between $|J^+_{\perp(m=n)}|$ and $|J^-_{\perp(m=n)}|$, we square both terms as

$$
\begin{aligned}
\left|J^+_{\perp(m=n)}\right|^2 &= \left\{J^+_m \exp\left[ik_{\parallel(m=n)}\right] + J^-_n \exp\left[-ik_{\parallel(m=n)}\right]\right\}\left\{J^+_m \exp\left[-ik_{\parallel(m=n)}\right] + J^-_n \exp\left[ik_{\parallel(m=n)}\right]\right\} \\
&= (J^+_m)^2 + (J^-_n)^2 + J^+_m J^-_n \exp\left[-2ik_{\parallel(m=n)}\right] + J^+_m J^-_n \exp\left[2ik_{\parallel(m=n)}\right],
\end{aligned}
\tag{A2}
$$

$$
\begin{aligned}
\left|J^-_{\perp(m=n)}\right|^2 &= \left\{J^-_m \exp\left[-ik_{\parallel(m=n)}\right] + J^+_n \exp\left[ik_{\parallel(m=n)}\right]\right\}\left\{J^-_m \exp\left[ik_{\parallel(m=n)}\right] + J^+_n \exp\left[-ik_{\parallel(m=n)}\right]\right\} \\
&= (J^-_m)^2 + (J^+_n)^2 + J^-_m J^+_n \exp\left[-2ik_{\parallel(m=n)}\right] + J^-_m J^+_n \exp\left[2ik_{\parallel(m=n)}\right].
\end{aligned}
\tag{A3}
$$

Comparing coefficients of different powers of $\exp[ik_{\parallel(m=n)}]$, we find that the requirements of $|J^+_{\perp(m=n)}| = |J^-_{\perp(m=n)}|$ can be expressed as

$$
(J^+_m)^2 + (J^-_n)^2 = (J^-_m)^2 + (J^+_n)^2, \quad J^+_m J^-_n = J^-_m J^+_n.
\tag{A4}
$$

Based on the identical principle of bosons, it is easy to know that Eq. (A4) is always satisfied. Hence, no skin state exists in this 3D subspace toward the 2D effective boundary.

Then we consider the 2D subspace of two bosons located at the same lattice site ($m = n \neq q$), and the effective boundary corresponds to the 1D subspace with all three bosons occupying the same lattice site ($m = n = q$). We express the corresponding Bloch Hamiltonian perpendicular to the effective 1D boundary ($m = n = q$) as

$$
\begin{aligned}
H\left[k_{\perp(m=n=q)}\right] &= J^\pm_m \exp(\pm ik_m) + J^\pm_n \exp(\pm ik_n) + J^\pm_q \exp(\pm iq) \\
&= \left\{J^\pm_m \exp\left[\pm ik_{\perp(m=n)}\right] + J^\pm_n \exp\left[\mp ik_{\perp(m=n)}\right]\right\} \exp\left[\pm ik_{\parallel(m=n)}\right] + J^\pm_q \exp(\pm iq) \\
&= J^\pm_{\parallel(m=n)} \exp\left[\pm ik_{\parallel(m=n)}\right] + J^\pm_q \exp(\pm iq) \\
&= \left\{J^\pm_{\parallel(m=n)} \exp\left[\pm ik_{\parallel(m=n=q)}\right] + J^\mp_q \exp\left[\mp ik_{\parallel(m=n=q)}\right]\right\} \exp\left[\pm ik_{\perp(m=n=q)}\right] \\
&= J^\pm_{\perp(m=n=q)} \exp\left[\pm ik_{\perp(m=n=q)}\right].
\end{aligned}
\tag{A5}
$$

Squaring both terms of $|J^\pm_{\perp(m=n=q)}|$, then we get

$$
\begin{aligned}
\left|J^+_{\perp(m=n=q)}\right|^2 &= (J^+_m)^2 + J^+_m J^+_n \left\{\exp\left[-2ik_{\perp(m=n)}\right] + \exp\left[2ik_{\perp(m=n)}\right]\right\} + (J^+_n)^2 + (J^-_q)^2 \\
&\quad + \left\{J^+_m \exp\left[ik_{\perp(m=n)}\right] + J^+_n \exp\left[-ik_{\perp(m=n)}\right]\right\}J^-_q \exp\left[2ik_{\parallel(m=n=q)}\right] \\
&\quad + \left\{J^+_m \exp\left[-ik_{\perp(m=n)}\right] + J^+_n \exp\left[ik_{\perp(m=n)}\right]\right\}J^-_q \exp\left[-2ik_{\parallel(m=n=q)}\right],
\end{aligned}
\tag{A6}
$$

$$
\begin{aligned}
\left|J^-_{\perp(m=n=q)}\right|^2 &= (J^-_m)^2 + J^-_m J^-_n \left\{\exp\left[2ik_{\perp(m=n)}\right] + \exp\left[-2ik_{\perp(m=n)}\right]\right\} + (J^-_n)^2 + (J^+_q)^2 \\
&\quad + \left\{J^-_m \exp\left[-ik_{\perp(m=n)}\right] + J^-_n \exp\left[ik_{\perp(m=n)}\right]\right\}J^+_q \exp\left[-2ik_{\parallel(m=n=q)}\right] \\
&\quad + \left\{J^-_m \exp\left[ik_{\perp(m=n)}\right] + J^-_n \exp\left[-ik_{\perp(m=n)}\right]\right\}J^+_q \exp\left[2ik_{\parallel(m=n=q)}\right].
\end{aligned}
\tag{A7}
$$

Comparing coefficients of different powers of $\exp[ik_{\parallel(m=n=q)}]$, we find that the requirements for realizing $|J^+_{\perp(m=n=q)}| = |J^-_{\perp(m=n=q)}|$ can be expressed as

$$
(J^+_m)^2 + (J^+_n)^2 + (J^-_q)^2 = (J^-_m)^2 + (J^-_n)^2 + (J^+_q)^2, \quad J^+_m J^+_n = J^-_m J^-_n, \quad \text{and} \quad J^+_{m,n} J^-_q = J^-_{m,n} J^+_q.
\tag{A8}
$$

Based on the identical principle of bosons, we conclude that Eq. (A8) cannot be satisfied, meaning skin states could exist in this 2D subspace toward the effective 1D boundary. In addition, in the Hermitian limit of three-boson system with $J^+_m = J^-_m$, $J^+_n = J^-_n$, $J^+_q = J^-_q$, we can see that Eq. (A8) is always satisfied, making the asymmetric coupling strength along the interaction-induced effective wall disappear. In this case, the strong interaction-induced aggregation effects cannot exist in the Hermitian system.

APPENDIX B: ANALYTICAL DERIVATION OF REQUIREMENTS FOR NON-HERMITIAN AGGREGATION EFFECTS OF *N* BOSONS

In this appendix, we generalize the interaction-induced non-Hermitian aggregation effects to the *N*-boson system. For universality, we consider the subspace with two bosonic clusters located at different lattice sites, where *P* bosons (marked from N_1 to N_P) are located at one lattice site and *O* bosons (marked from N_{1+P} to N_{O+P}) are located at another lattice site. Here, we have $(P, O) \propto \{1, \ldots, N\}$.

First, we consider the system under the restriction of $P = O$. In this case, we express the N-boson Bloch Hamiltonian perpendicular to the effective boundary, which corresponds to the state with $P + O$ bosons located in the same lattice, as

$$H\big[k_{\perp(N_1=\cdots=N_{O+P})}\big] = J^{\pm}_{\perp(N_1=\cdots=N_{O+P})}\exp\big[\pm ik_{\perp(N_1=\cdots=N_{O+P})}\big], \tag{B1}$$

where $J^{\pm}_{\perp(N_1=\cdots=N_{O+P})} = J^{\pm}_{\|(N_1=\cdots=N_P)}\exp[\pm ik_{\|(N_1=\cdots=N_{O+P})}] + J^{\mp}_{\|(N_{1+P}=\cdots=N_{O+P})}\exp[\mp ik_{\|(N_1=\cdots=N_{O+P})}]$ are the effective hopping strengths along $\pm\mathbf{k}_{\perp(N_1=\cdots=N_{O+P})}$. Moreover, the hopping amplitudes $J^{\pm}_{\|(N_1=\cdots=N_P)}$ and $J^{\pm}_{\|(N_{1+P}=\cdots=N_{O+P})}$ are expressed as

$$
\begin{aligned}
J^{\pm}_{\|(N_1=\cdots=N_P)} = {} & J^{\pm}_{N_1}\exp\big[\pm ik_{\perp(N_1=N_2)}\big]\exp\big[\pm ik_{\perp(N_1=N_2=N_3)\ldots}\big]\exp\big[\pm ik_{\perp(N_1=\cdots=N_P)}\big] \\
& + J^{\pm}_{N_2}\exp\big[\mp ik_{\perp(N_1=N_2)}\big]\exp\big[\pm ik_{\perp(N_1=N_2=N_3)\ldots}\big]\exp\big[\pm ik_{\perp(N_1=\cdots=N_P)}\big] \\
& + J^{\pm}_{N_3}\exp\big[\mp ik_{\perp(N_1=N_2=N_3)}\big]\exp\big[\pm ik_{\perp(N_1=N_2=N_3=N_4)\ldots}\big]\exp\big[\pm ik_{\perp(N_1=\cdots=N_P)}\big] \\
& + J^{\pm}_{N_4}\exp\big[\mp ik_{\perp(N_1=N_2=N_3=N_4)}\big]\exp\big[\pm ik_{\perp(N_1=N_2=N_3=N_4=N_5)\ldots}\big]\exp\big[\pm ik_{\perp(N_1=\cdots=N_P)}\big] \\
& + \cdots + J^{\pm}_{(N_P-1)}\exp\big[\mp ik_{\perp(N_1=\cdots=N_{P-1})}\big]\exp\big[\pm ik_{\perp(N_1=\cdots=N_P)}\big] \\
& + J^{\pm}_{N_P}\exp\big[\mp ik_{\perp(N_1=\cdots=N_P)}\big],
\end{aligned}
\tag{B2}
$$

$$
\begin{aligned}
J^{\pm}_{\|(N_{P+1}=\cdots=N_{P+O})} = {} & J^{\pm}_{N_{P+1}}\exp\big[\pm ik_{\perp(N_{P+1}=N_{P+2})}\big]\ldots\exp\big[\pm ik_{\perp(N_{P+1}=\cdots=N_{P+O})}\big] \\
& + J^{\pm}_{N_{P+2}}\exp\big[\mp ik_{\perp(N_{P+1}=N_{P+2})}\big]\exp\big[\pm ik_{\perp(N_{P+1}=N_{P+2}=N_{P+3})\ldots}\big]\exp\big[\pm ik_{\perp(N_{P+1}=\cdots=N_{P+o})}\big] \\
& + J^{\pm}_{N_{P+3}}\exp\big[\mp ik_{\perp(N_{P+1}=N_{P+2}=N_{P+3})}\big]\exp\big[\pm ik_{\perp(N_{P+1}=N_{P+2}=N_{P+3}=N_{P+4})\ldots}\big]\exp\big[\pm ik_{\perp(N_{P+1}=\cdots=N_{P+O})}\big] \\
& + J^{\pm}_{N_{P+4}}\exp\big[\mp ik_{\perp(N_{P+1}=N_{P+2}=N_{P+3}=N_{P+4})}\big]\exp\big[\pm ik_{\perp(N_{P+1}=N_{P+2}=N_{P+3}=N_{P+4}=N_{P+5})\ldots}\big] \\
& \times \exp\big[\pm ik_{\perp(N_{P+1}=\cdots=N_{P+O})}\big] \\
& + \cdots + J^{\pm}_{N_{P+O-1}}\exp\big[\mp ik_{\perp(N_{P+1}=\cdots=N_{P+O-1})}\big]\exp\big[\pm ik_{\perp(N_{P+1}=\cdots=N_{P+O})}\big] \\
& + J^{\pm}_{N_{P+O}}\exp\big[\mp ik_{\perp(N_{P+1}=\cdots=N_{P+O})}\big].
\end{aligned}
\tag{B3}
$$

In this case, the following expressions must be satisfied to make $|J^{+}_{\perp(N_1=\cdots=N_{O+P})}| = |J^{-}_{\perp(N_1=\cdots=N_{O+P})}|$:

$$
\begin{aligned}
\sum_{i=[N_1,\,N_P]}(J_i^+)^2 + \sum_{j=[N_{P+1},N_{P+o}]}(J_j^-)^2 &= \sum_{i=[N_1,\,N_P]}(J_i^-)^2 + \sum_{j=[N_{P+1},N_{P+o}]}(J_j^+)^2, \\
J_i^+ J_j^+ + J_k^- J_l^- &= J_i^- J_j^- + J_k^+ J_l^+ \quad\text{with}\quad i \neq j \propto [N_1,\,N_p], \quad k \neq l \propto [N_{P+1}, N_{P+O}], \\
J_i^- J_k^+ &= J_i^+ J_k^- \quad\text{with}\quad i \propto [N_1,\,N_P], \quad k \propto [N_{P+1}, N_{P+O}].
\end{aligned}
\tag{B4}
$$

Under the limitation of identical principle of bosons, Eq. (B4) is always satisfied. Hence, the non-Hermitian aggregation effects cannot appear in the subspace toward the effective boundary with $P = O$.

Then we focus on the N-boson system with $P \neq O$. Similarly, referring to Eqs. (B1)–(B3), the requirement of symmetric hopping strengths with $P < O$ can be expressed as

$$
\begin{aligned}
\sum_{i=[N_1,\,N_P]}(J_i^+)^2 + \sum_{j=[N_{P+1},N_{P+o}]}(J_j^-)^2 &= \sum_{i=[N_1,\,N_P]}(J_i^-)^2 + \sum_{j=[N_{P+1},N_{P+o}]}(J_j^+)^2, \\
J_i^+ J_j^+ + J_k^- J_l^- &= J_i^- J_j^- + J_k^+ J_l^+ \quad\text{with}\quad i \neq j \propto [N_1,\,N_P], \quad k \neq l \propto [N_{P+1}, N_{P+P}], \\
J_k^+ J_l^+ &= J_k^- J_l^- \quad\text{with}\quad k \propto [N_{P+1}, N_{P+P}] \quad\text{and}\quad l \propto [N_{P+P+1}, N_{P+O}], \\
J_i^- J_k^+ &= J_i^+ J_k^- \quad\text{with}\quad i \propto [N_1,\,N_P], \quad k \propto [N_{P+1}, N_{P+O}].
\end{aligned}
\tag{B5}
$$

Using the exchange symmetry of the multiboson wave function, Eq. (B5) can be rewritten as

$$
\begin{aligned}
\sum_{i=[N_1,\,N_P]}(J_i^+)^2 + \sum_{j=[N_{P+1},N_{P+o}]}(J_j^-)^2 &= \sum_{i=[N_1,\,N_P]}(J_i^-)^2 + \sum_{j=[N_{P+1},N_{P+o}]}(J_j^+)^2, \\
J_i^+ J_j^+ + J_k^- J_l^- &= J_i^- J_j^- + J_k^+ J_l^+ \quad\text{with}\quad i \neq j \propto [N_1,\,N_P], \quad k \neq l \propto [N_{P+1}, N_{P+O}], \\
J_k^+ J_l^+ &= J_k^- J_l^- \quad\text{with}\quad k \neq l \propto [N_{P+1}, N_{P+O}], \\
J_i^- J_k^+ &= J_i^+ J_k^- \quad\text{with}\quad i \propto [N_1,\,N_P], \quad k \propto [N_{P+1}, N_{P+O}].
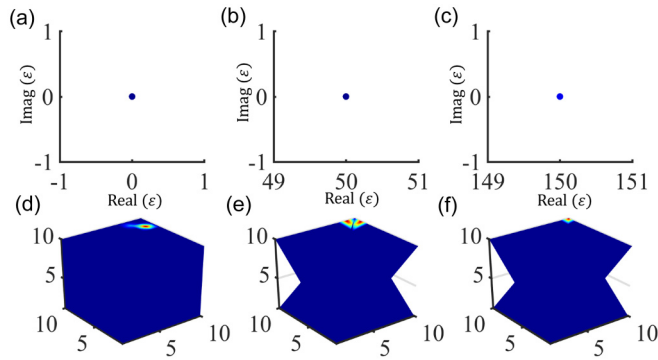\end{aligned}
\tag{B6}
$$

FIG. 4. Numerical results of three bosons in the one-dimensional (1D) chain with open boundaries. (a)–(c) Results of the complex energy spectra of the three-boson system in three subspaces with different energies and dimensions. The blue color corresponds to the localized eigenstates quantified by the *PR*. (d)–(f) Illustrations of the profiles of normalized density of states in three subspaces.

Under the limitation of the identical principle of bosons, we know that Eq. (B6) cannot be satisfied. Hence, interaction-induced skin states in Hilbert space (non-Hermitian aggregation effects) can appear in the subspace toward the effective boundary with nonidentical occupation $P \neq O$.

APPENDIX C: NUMERICAL RESULTS OF THE THREE-BOSON SYSTEM WITH OPEN BOUNDARIES AND DIFFERENT INTERACTION STRENGTHS AND LATTICE SIZES

In this appendix, we give more numerical results and discussion on the interaction-induced non-Hermitian aggregation effects with different boundaries conditions, interaction strengths, and lattice sizes.

At first, we show that the interaction-induced non-Hermitian aggregation effect could only appear in the three-boson lattice with PBCs. Under open boundary conditions, like the single-particle case, all correlated bosons accumulate at physical boundaries. To further illustrate this phenomenon, we calculate the complex energy spectra and profiles of density of states for the 1D three-boson system with open boundaries, as shown in Fig. 4. It is clearly shown that the eigenstates in each subspace are strongly localized around the zero-dimensional corner.

Then we study the influence of onsite interaction strengths on non-Hermitian aggregation effects. As shown in Figs. 5(a)–5(d), we numerically calculate the complex energy spectra and the profile of the density of states for the 1D three-boson system with the interaction strength being $U = 40, 20, 10,$ and 5. Other parameters are set as $J^+ = -1$, $J^- = 0$, and $L = 10$. Like the result shown in the main text, the skin state in Hilbert space only appears in the 2D subspace with different interaction energies. Moreover, based on the calculated PR and $\psi_d(m, n, q)$, we can see that the localization in Hilbert space is significantly influenced by the interaction energy, where the localization degree of skin states in the 2D subspace decreases with the interaction energy becoming weaker. This is because the coupling strength of probability amplitudes in different subspaces increases with decreasing the onsite interaction energy, making the effective boundary much fuzzier than the case with the strong interaction. To further quantify the localization for the skin state in Hilbert space with different interaction strengths, we calculate the average PR of all eigenmodes in the 2D energy sector [around U in Fig. 2(b)], where two bosons locate at a single site and the remaining one locates at another site, as shown in Fig. 5(e). Here, we set $L = 10$. We can see that the average PR approaches a constant with increasing the interaction energy.
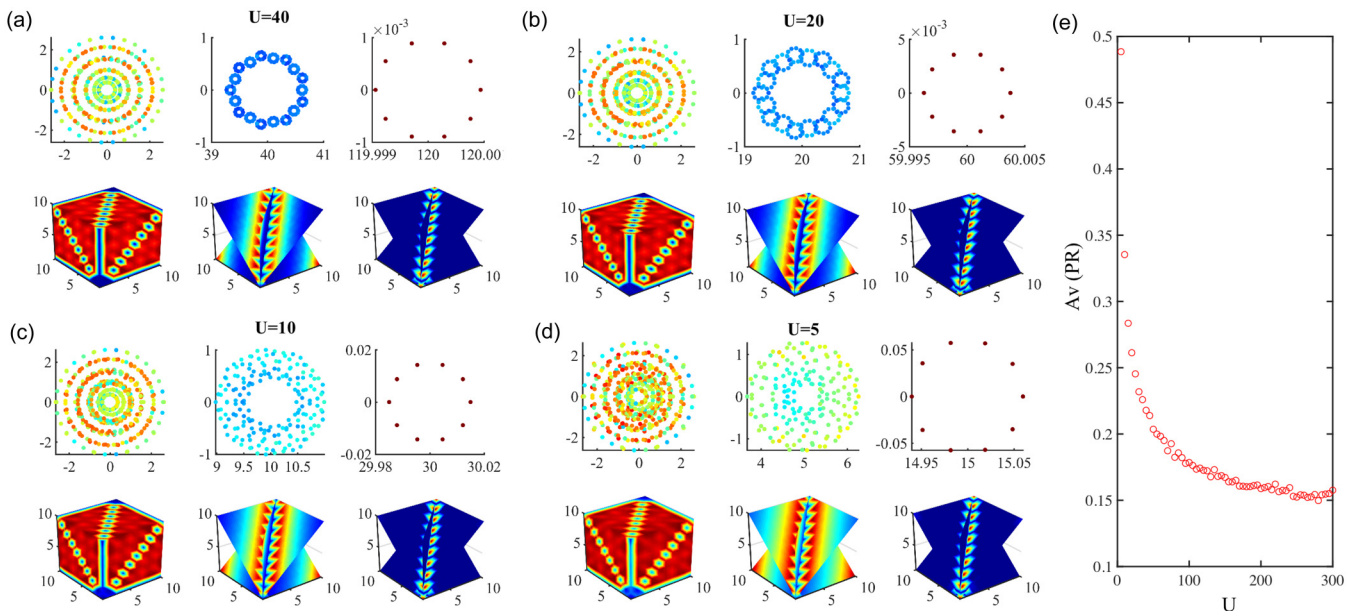

FIG. 5. (a)–(d) present the complex energy spectra and the profile of the density of states for the one-dimensional (1D) three-boson system with the interaction strength being $U = 40, 20, 10,$ and 5, respectively. Other parameters are set as $J^+ = -1$, $J^- = 0$, and $L = 10$. (e) The calculated the average participation ratio (PR) of all eigenmodes in the energy sector [around U in Fig. 2(b)] with different interaction strengths.
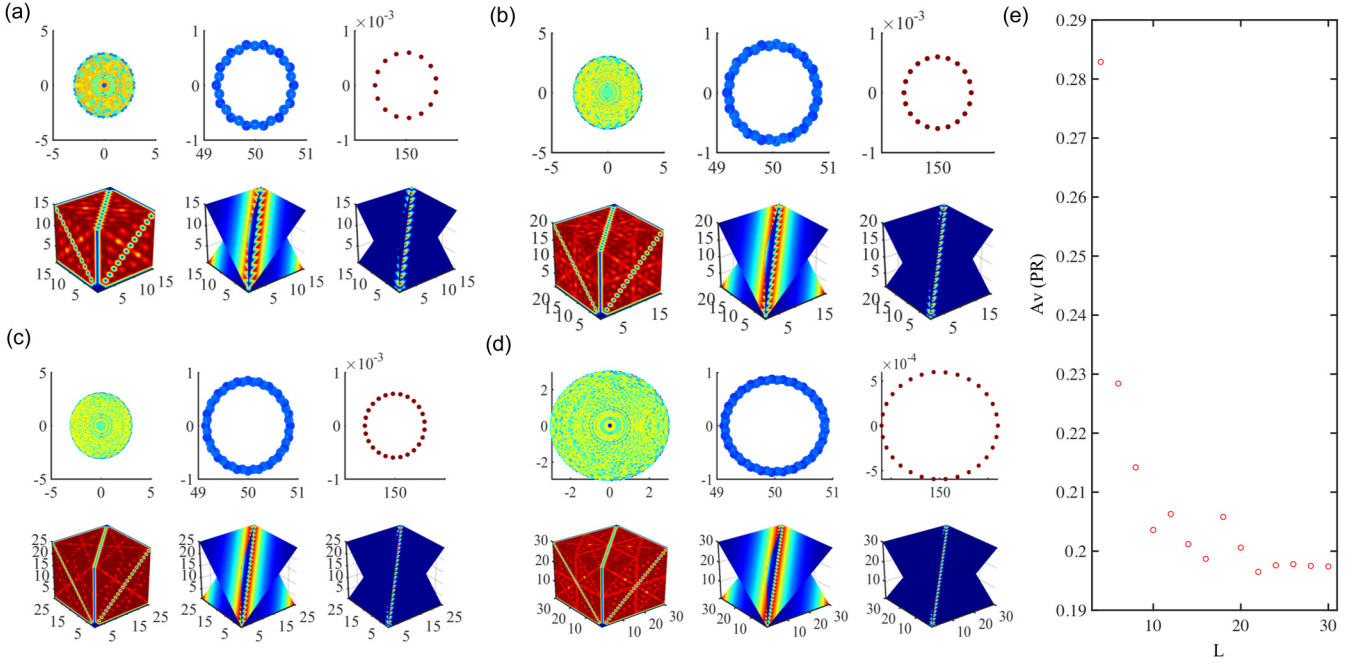
FIG. 6. (a)–(d) present the complex energy spectra and the profile of the density of states for the one-dimensional (1D) three-boson system with lattice sizes of $L = 15$, 20, 25, and 30, respectively. Other parameters are set as $J^+ = -1$, $J^- = 0$, and $U = 50$. (e) The calculated the average participation ratio (PR) of all eigenmodes in the energy sector [around U in Fig. 2(b)] with different lattice sizes.

Finally, we give numerical results of three bosons with different lattice sizes. As shown in Figs. 6(a)–6(d), we numerically calculate the complex energy spectra and the profile of the density of states for the 1D three-boson system with lattice lengths of $L = 15$, 20, 25, and 30. Other parameters are set as $J^+ = -1$, $J^- = 0$, and $U = 50$. Like the results shown in the main text, the skin effect always appears in the 2D subspace with different lattice lengths. To quantify the localization for the skin state in Hilbert space with different lattice sizes, we calculate the average PR of all eigenmodes in the 2d energy sector (around U), as shown in Fig. 6(e). Here, we set $U = 50$. It is found that the localization strength of skin states (averaged PR) saturates with increasing the lattice size, indicating the exponential decay of skin states in the Hilbert space.

APPENDIX D: ANALYTICAL AND NUMERICAL RESULTS OF THE FOUR- AND FIVE-BOSON SYSTEMS

To further prove the analytical results of the N-body bosonic system discussed above, in the following, we will give both numerical and analytical results of two examples, which contain subspaces with $P = O > 1$ and $P \neq O > 1$, respectively. First, a simple case with $N = 4$ is considered, and we focus on the 2D subspace with $P = O = 2$. In this case, the four-boson Bloch Hamiltonian (with $m = n \neq q = p$) can be expressed in the form of a single-particle Hatano-Nelson chain perpendicular to the effective 1D boundary ($m = n = q = p$) as

$$
\begin{aligned}
H\big[k_{\perp(m=n=q=p)}\big] &= J_m^\pm \exp\left(\pm ik_m\right) + J_n^\pm \exp\left(\pm ik_n\right) + J_q^\pm \exp\left(\pm iq\right) + J_p^\pm \exp\left(\pm ip\right) \\
&= \left\{J_m^\pm \exp\left[\pm ik_{\perp(m=n)}\right] + J_n^\pm \exp\left[\mp ik_{\perp(m=n)}\right]\right\} \exp\left[\pm ik_{\parallel(m=n)}\right] \\
&\quad + \left\{J_q^\pm \exp\left[\pm ik_{\perp(q=p)}\right] + J_p^\pm \exp\left[\mp ik_{\perp(q=p)}\right]\right\} \exp\left[\pm ik_{\parallel(q=p)}\right] \\
&= J_{\parallel(m=n)}^\pm \exp\left[\pm ik_{\parallel(m=n)}\right] + J_{\parallel(q=p)}^\pm \exp\left[\pm ik_{\parallel(q=p)}\right] \\
&= \left\{J_{\parallel(m=n)}^\pm \exp\left[\pm ik_{\parallel(m=n=q=p)}\right] + J_{\parallel(q=p)}^\mp \exp\left[\mp ik_{\parallel(m=n=q=p)}\right]\right\} \exp\left[\pm ik_{\perp(m=n=q=p)}\right] \\
&= J_{\perp(m=n=q=p)}^\pm \exp\left[\pm ik_{\perp(m=n=q=p)}\right].
\end{aligned}
\tag{D1}
$$

Squaring both terms of $|J_{\perp(m=n=q=p)}^\pm|$, then we get

$$
\begin{aligned}
\left|J_{\perp(m=n=q=p)}^+\right|^2 &= (J_m^+)^2 + (J_n^+)^2 + (J_q^-)^2 + (J_p^-)^2 + J_m^+ J_n^+ \left\{\exp\left[-2ik_{\perp(m=n)}\right] + \exp\left[2ik_{\perp(m=n)}\right]\right\} \\
&\quad + J_q^- J_p^- \left\{\exp\left[-2ik_{\perp(p=q)}\right] + \exp\left[2ik_{\perp(p=q)}\right]\right\} + \left\{J_m^+ \exp\left[ik_{\perp(m=n)}\right] + J_n^+ \exp\left[-ik_{\perp(m=n)}\right]\right\} \\
&\quad \times \left\{J_q^- \exp\left[ik_{\perp(q=p)}\right] + J_p^- \exp\left[-ik_{\perp(q=p)}\right]\right\} \exp\left[2ik_{\parallel(m=n=q=p)}\right] + \left\{J_m^+ \exp\left[-ik_{\perp(m=n)}\right] + J_n^+ \exp\left[ik_{\perp(m=n)}\right]\right\} \\
&\quad \times \left\{J_q^- \exp\left[-ik_{\perp(q=p)}\right] + J_p^- \exp\left[ik_{\perp(q=p)}\right]\right\} \exp\left[-2ik_{\parallel(m=n=q=p)}\right],
\end{aligned}
\tag{D2}
$$

$$\left|J^-_{\perp(m=n=q=p)}\right|^2 = (J^-_m)^2 + (J^-_n)^2 + (J^+_q)^2 + (J^+_p)^2 + J^-_m J^-_n \left\{\exp\left[-2ik_{\perp(m=n)}\right] + \exp\left[2ik_{\perp(m=n)}\right]\right\}$$
$$+ J^+_q J^+_p \left\{e\left[-2ik_{\perp(p=q)}\right] + \exp\left[2ik_{\perp(p=q)}\right]\right\} + \left\{J^-_m \exp\left[ik_{\perp(m=n)}\right] + J^-_n \exp\left[-ik_{\perp(m=n)}\right]\right\}$$
$$\times \left\{J^+_q \exp\left[ik_{\perp(q=p)}\right] + J^+_p \exp\left[-ik_{\perp(q=p)}\right]\right\} \exp\left[2ik_{\parallel(m=n=q=p)}\right] + \left\{J^-_m \exp\left[-ik_{\perp(m=n)}\right] + J^-_n \exp\left[ik_{\perp(m=n)}\right]\right\}$$
$$\times \left\{J^+_q \exp\left[-ik_{\perp(q=p)}\right] + J^+_p \exp\left[ik_{\perp(q=p)}\right]\right\} \exp\left[-2ik_{\parallel(m=n=q=p)}\right]. \tag{D3}$$

The requirements for realizing the relationship of $|J^+_{\perp(m=n=q=p)}| = |J^-_{\perp(m=n=q=p)}|$ can be expressed as

$$(J^+_m)^2 + (J^+_n)^2 + (J^-_q)^2 + (J^-_p)^2 = (J^-_m)^2 + (J^-_n)^2 + (J^+_q)^2 + (J^+_p)^2,$$
$$J^+_m J^+_n + J^-_q J^-_p = J^-_m J^-_n + J^+_q J^+_p, \quad J^+_{m,n} J^-_{q,p} = J^-_{m,n} J^+_{q,p}. \tag{D4}$$

Based on the identical principle of bosons, we know that Eq. (D4) is always satisfied. Hence, no skin states exist in the four-boson subspace with $P = O = 2$.

We numerically calculate the complex energy spectra and PR of the 1D four-boson system. The parameters used are set as $J^+ = -1$, $J^- = 0$, $U = 50$, and $L = 9$. Figures 7(a)–7(e) present the energy spectra of five subspaces with different energies and dimensions. The first subspace [in Fig. 7(a)] corresponds to the state with all four bosons located at different lattice sites, and the associated eigenenergy is approximately $\varepsilon \sim 0$. The second subspace [in Fig. 7(b)] corresponds to the state with only two bosons located in the same lattice, and the associated eigenenergy is approximately $\varepsilon \sim U$. The third subspace [in Fig. 7(c)] corresponds to the state with two bosons located at the same lattice site and the other two bosons located at another lattice site. In this case, the associated eigenenergy is approximately $\varepsilon \sim 2U$. The fourth and fifth

subspaces [in Figs. 7(d) and 7(e)] correspond to states with three and four bosons located at the same lattice site, and the corresponding eigenenergies are approximately $\varepsilon \sim 3U$ and $\varepsilon \sim 6U$, respectively. As clearly shown in Figs. 7(a) and 7(c), the PR does not exhibit localization behavior with identical occupations of four bosons. Hence, there is no skin effect in subspaces with $P = O = 1$ and $P = O = 2$. Moreover, when the subspace sustains different bosonic clusters (nonidentical occupations), as shown in Fig. 7(b) ($P = 1$ and $O = 2$) and Fig. 7(d) ($P = 1$ and $O = 3$), the interaction-induced skin state in Hilbert space could appear.

Then we give another example of the five-boson system, where a 2D subspace with $P = 2$ and $O = 3$ exists. In this case, the five-boson Bloch Hamiltonian in the 2D subspace ($m = n \neq q = p = o$) could be expressed in the form of a single-particle Hatano-Nelson chain perpendicular to the effective 1D boundary ($m = n = q = p = o$) as

$$H\left[k_{\perp(m=n=q=p=o)}\right] = J^\pm_m \exp(\pm ik_m) + J^\pm_n \exp(\pm ik_n) + J^\pm_q \exp[\pm iq] + J^\pm_p \exp(\pm ip) + J^\pm_o \exp(\pm io)$$
$$= \left\{J^\pm_m e\left[\pm ik_{\perp(m=n)}\right] + J^\pm_n \exp\left[\mp ik_{\perp(m=n)}\right]\right\} \exp\left[\pm ik_{\parallel(m=n)}\right]$$
$$+ \left(\left\{J^\pm_q \exp\left[\pm ik_{\perp(q=p)}\right] + J^\pm_p \exp\left[\mp ik_{\perp(q=p)}\right]\right\} \exp\left[\pm ik_{\perp(q=p=o)}\right]\right.$$
$$\left. + J^\pm_o \exp\left[\mp ik_{\perp(q=p=o)}\right]\right) \exp\left[\pm ik_{\parallel(q=p=o)}\right]$$
$$= J^\pm_{\parallel(m=n)} \exp\left[\pm ik_{\parallel(m=n)}\right] + J^\pm_{\parallel(q=p=o)} \exp\left[\pm ik_{\parallel(q=p=o)}\right]$$
$$= \left\{J^\pm_{\parallel(m=n)} \exp\left[\pm ik_{\parallel(m=n=q=p=o)}\right] + J^\mp_{\parallel(q=p=o)} \exp\left[\mp ik_{\parallel(m=n=q=p=o)}\right]\right\} \exp\left[\pm ik_{\perp(m=n=q=p=o)}\right]$$
$$= J^\pm_{\perp(m=n=q=p=o)} \exp\left[\pm ik_{\perp(m=n=q=p=o)}\right]. \tag{D5}$$

Squaring both terms of $|J^\pm_{\perp(m=n=q=p=o)}|$, then we get

$$\left|J^+_{\perp(m=n=q=p=o)}\right|^2 = (J^+_m)^2 + (J^+_n)^2 + (J^-_q)^2 + (J^-_p)^2 + (J^-_o)^2 + J^+_m J^+_n \left\{\exp\left[-2ik_{\perp(m=n)}\right] + \exp\left[2ik_{\perp(m=n)}\right]\right\}$$
$$+ J^-_q J^-_p \left\{\exp\left[-2ik_{\perp(p=q)}\right] + \exp\left[2ik_{\perp(p=q)}\right]\right\}$$
$$+ J^-_q J^-_o \left(\exp\left\{-\left[2ik_{\perp(q=p=o)} + k_{\perp(q=p)}\right]\right\} + \exp\left[2ik_{\perp(q=p=o)} + k_{\perp(q=p)}\right]\right)$$
$$+ J^-_p J^-_o \left(\exp\left\{-\left[2ik_{\perp(q=p=o)} - k_{\perp(q=p)}\right]\right\} + \exp\left[2ik_{\perp(q=p=o)} - k_{\perp(q=p)}\right]\right)$$
$$+ J^+_m J^-_q \left(\exp\left\{i\left[k_{\perp(m=n)} + k_{\perp(q=p)} + k_{\perp(q=p=o)}\right]\right\} + \exp\left\{-i\left[k_{\perp(m=n)} + k_{\perp(q=p)} + k_{\perp(q=p=o)}\right]\right\}\right)$$
$$+ J^+_m J^-_p \left(\exp\left\{i\left[k_{\perp(m=n)} - k_{\perp(q=p)} + k_{\perp(q=p=o)}\right]\right\} + \exp\left\{-i\left[k_{\perp(m=n)} - k_{\perp(q=p)} + k_{\perp(q=p=o)}\right]\right\}\right)$$
$$+ J^+_m J^-_o \left(\exp\left\{i\left[k_{\perp(m=n)} - k_{\perp(q=p=o)}\right]\right\} + \exp\left\{-i\left[k_{\perp(m=n)} - k_{\perp(q=p=o)}\right]\right\}\right)$$
$$+ J^+_n J^-_q \left(\exp\left\{i\left[-k_{\perp(m=n)} + k_{\perp(q=p)} + k_{\perp(q=p=o)}\right]\right\}\right.$$

$$+ \exp\left\{-i\left[-k_{\perp(m=n)} + k_{\perp(q=p)} + k_{\perp(q=p=o)}\right]\right\}\right) + J_n^+ J_p^- \left(\exp\left\{i\left[-k_{\perp(m=n)} - k_{\perp(q=p)} + k_{\perp(q=p=o)}\right]\right\}\right.$$

$$\left. + \exp\left\{-i\left[-k_{\perp(m=n)} - k_{\perp(q=p)} + k_{\perp(q=p=o)}\right]\right\}\right)$$

$$+ J_n^+ J_o^- \left(\exp\left\{i\left[-k_{\perp(m=n)} - k_{\perp(q=p=o)}\right]\right\} + \exp\left\{-i\left[-k_{\perp(m=n)} - k_{\perp(q=p=o)}\right]\right\}\right), \tag{D6}$$

$$\left|J_{\perp(m=n=q=p=o)}^-\right|^2 = (J_m^-)^2 + (J_n^-)^2 + (J_q^-)^2 + (J_p^+)^2 + (J_o^+)^2 + J_m^- J_n^- \left\{\exp\left[-2ik_{\perp(m=n)}\right] + \exp\left[2ik_{\perp(m=n)}\right]\right\}$$

$$+ J_q^+ J_p^+ \left\{\exp\left[-2ik_{\perp(p=q)}\right] + \exp\left[2ik_{\perp(p=q)}\right]\right\}$$

$$+ J_q^+ J_o^+ \left(\exp\left\{-\left[2ik_{\perp(q=p=o)} + k_{\perp(q=p)}\right]\right\} + \exp\left[2ik_{\perp(q=p=o)} + k_{\perp(q=p)}\right]\right)$$

$$+ J_p^+ J_o^+ \left(\exp\left\{-\left[2ik_{\perp(q=p=o)} - k_{\perp(q=p)}\right]\right\} + \exp\left[2ik_{\perp(q=p=o)} - k_{\perp(q=p)}\right]\right)$$

$$+ J_m^- J_q^+ \left(\exp\left\{i\left[k_{\perp(m=n)} + k_{\perp(q=p)} + k_{\perp(q=p=o)}\right]\right\} + \exp\left\{-i\left[k_{\perp(m=n)} + k_{\perp(q=p)} + k_{\perp(q=p=o)}\right]\right\}\right)$$

$$+ J_m^- J_p^+ \left(\exp\left\{i\left[k_{\perp(m=n)} - k_{\perp(q=p)} + k_{\perp(q=p=o)}\right]\right\} + \exp\left\{-i\left[k_{\perp(m=n)} - k_{\perp(q=p)} + k_{\perp(q=p=o)}\right]\right\}\right)$$

$$+ J_m^- J_o^+ \left(\exp\left\{i\left[k_{\perp(m=n)} - k_{\perp(q=p=o)}\right]\right\} + \exp\left\{-i\left[k_{\perp(m=n)} - k_{\perp(q=p=o)}\right]\right\}\right)$$

$$+ J_n^- J_q^+ \left(\exp\left\{i\left[-k_{\perp(m=n)} + k_{\perp(q=p)} + k_{\perp(q=p=o)}\right]\right\} + \exp\left\{-i\left[-k_{\perp(m=n)} + k_{\perp(q=p)} + k_{\perp(q=p=o)}\right]\right\}\right)$$

$$+ J_n^- J_p^+ \left(\exp\left\{i\left[-k_{\perp(m=n)} - k_{\perp(q=p)} + k_{\perp(q=p=o)}\right]\right\} + \exp\left\{-i\left[-k_{\perp(m=n)} - k_{\perp(q=p)} + k_{\perp(q=p=o)}\right]\right\}\right)$$

$$+ J_n^- J_o^+ \left(\exp\left\{i\left[-k_{\perp(m=n)} - k_{\perp(q=p=o)}\right]\right\} + \exp\left\{-i\left[-k_{\perp(m=n)} - k_{\perp(q=p=o)}\right]\right\}\right). \tag{D7}$$

Hence, the requirements for realizing the relationship of $|J_{\perp(m=n=q=p=o)}^+| = |J_{\perp(m=n=q=p=o)}^-|$ can be expressed as

$$(J_m^+)^2 + (J_n^+)^2 + (J_q^-)^2 + (J_p^-)^2 + (J_o^-)^2 = (J_m^-)^2 + (J_n^-)^2 + (J_q^+)^2 + (J_p^+)^2 + (J_o^+)^2,$$

$$J_m^+ J_n^+ + J_q^- J_p^- = J_m^- J_n^- + J_q^+ J_p^+,$$

$$J_q^+ J_o^+ = J_q^- J_o^-,$$

$$J_p^+ J_o^+ = J_p^- J_o^-,$$

$$J_{m,n}^+ J_{q,p,o}^- = J_{m,n}^- J_{q,p,o}^+. \tag{D8}$$

In this case, based on the identical principle of bosons, we know that Eq. (D8) cannot be satisfied. Hence, skin states exist in the 2D subspace with $P = 2$ and $O = 3$.

To prove the five-boson analytical result, we numerically calculate the complex energy spectra and *PR* of the 1D five-boson system. The parameters used are set as $J^+ = -1$, $J^- = 0$, $U = 50$, and $L = 6$. Figures 8(a)–8(g) present the energy spectra of seven subspaces. The first subspace [in Fig. 8(a)] corresponds to the state with all five bosons located at different lattices, and the associated eigenenergy is ~ 0. In this case, the identical occupation makes the skin state unable to appear. The second subspace [in Fig. 8(b)] corresponds to the state with only two bosons located in the same lattice, and the associated eigenenergy is $\sim U$. In this case, there is an unbalanced bosonic cluster ($P = 1$ and $O = 2$), and the skin state could appear toward the effective boundary; that is, three bosons are located at the same site. The third subspace [in Fig. 8(c)] corresponds to the state with a pair of two-boson clusters located at different lattice sites, where the associated eigenenergy is $\sim 2U$. In this case, there are unbalanced bosonic clusters ($P = 1$ and $O = 2$), and the skin state exists in this subspace. The fourth subspace [in Fig. 8(d)] corresponds to the state with only three bosons located at the same site, and the associated eigenenergy is $\sim 3U$. In this case, there are unbalanced bosonic clusters ($P = 1$ and $O = 3$),

and the skin state can also appear. The fifth subspace [in Fig. 8(e)] corresponds to the state with three bosons located at the same lattice site and the other two bosons located at another lattice site, where the associated eigenenergy is $\sim 4U$.
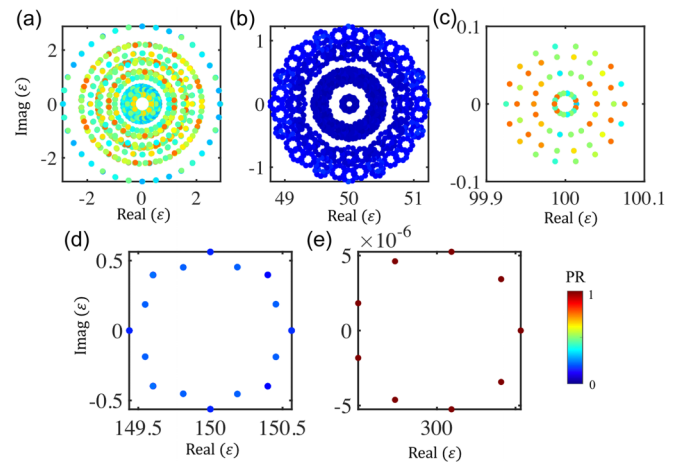

FIG. 7. (a)–(e) present the complex energy spectra and *PR* for five subspaces of the one-dimensional (1D) four-boson system, where the associated parameters are set as $J^+ = -1$, $J^- = 0$, $U = 50$, and $L = 9$.
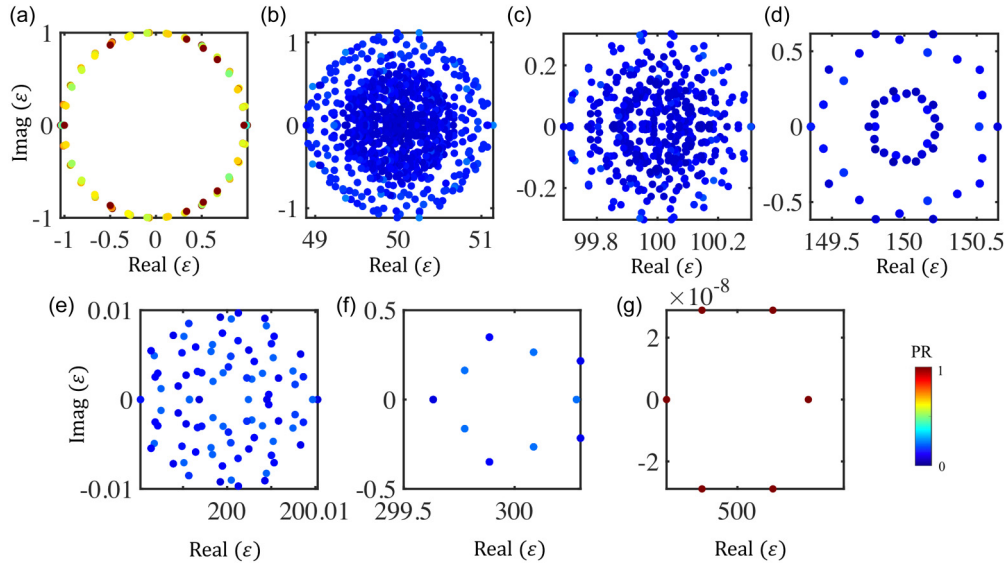
FIG. 8. (a)–(g) present the energy spectra of seven subspaces for the one-dimensional (1D) five-boson system with used parameters set as $J^+ = -1, J^- = 0, U = 50$, and $L = 6$.

In this case, there are unbalanced bosonic clusters ($P = 2$ and $O = 3$), and the skin state appears. The sixth and seventh subspaces [in Figs. 8(f) and 8(g)] correspond to states with four and five bosons located at the same lattice site, and the associated eigenenergies are $\sim 6U$ and $10U$, respectively. The sixth subspace possesses unbalanced bosonic clusters ($P = 1$ and $O = 4$), and the skin state could appear. From the above numerical calculations, we can conclude that all subspaces with unbalanced bosonic clusters (nonidentical occupations) can exhibit skin effects, which is consistent with the analytical prediction.

APPENDIX E: DETAILS FOR THE DERIVATION OF THE CIRCUIT EIGENEQUATION

In this appendix, we give a detailed derivation of the circuit eigenequation and the correspondence between the designed 3D circuit lattice and the 1D three-body Bose-Hubbard Hamiltonian. Ensured by the PBC, each circuit node (m, n, q) is connected with six adjacent nodes, where a capacitor C_1 and a one-way capacitor C_2 [being positive (negative) along the m ($-m$), n ($-n$), and q ($-q$) directions] are parallelly connected to realize nonreciprocal coupling between linked circuit nodes. Moreover, each circuit node is grounded by an inductor (L_g), and the extra capacitor C_U is grounded on the circuit nodes within diagonal planes ($m = n \neq q$, $m = q \neq n$, and $n = q \neq m$) to realize the effective onsite interaction. In this case, circuit nodes on the diagonal line (red nodes, $m = n = q$) are grounded by three C_U. Carrying out Kirchhoff's law on the circuit node (m, n, q), we obtain the following equation:

$$
I_{mnq} = i\omega^{-1} \Bigg\{ \left[-\frac{1}{L_g} + \omega^2 C_U (\delta_{mn} + \delta_{mq} + \delta_{nq}) \right] V_{mnq}
$$
$$
+ (C_1 \pm C_2)[(V_{mnq} - V_{m\pm1,n,q}) + (V_{mnq} - V_{m,n\pm1,n})
$$
$$
+ (V_{mnq} - V_{m,n,q\pm1})] \Bigg\}, \tag{E1}
$$

where I_{mnq} and V_mnq are the net current and voltage of node (m, n, q), and the voltage on the circuit node (m, n, q) is in the form of $V_{mnq}e^{i\omega t}$.

We assume that there is no external source, so that the current flowing out of the node is zero. In this case, Eq. (E1) becomes

$$
\left(\frac{f_0^2}{f^2} - 6 \right) V_{mnq} = -\frac{C_1 \pm C_3}{C_1} (V_{m\pm1,n,q} + V_{m,n\pm1,q} + V_{m,n,q\pm1})
$$
$$
+ \frac{C_U}{C_1} (\delta_{mn} + \delta_{mq} + \delta_{nq}) V_{mnq}, \tag{E2}
$$

with $f_0 = 1/2\pi \sqrt{C_1 L_g}$. We provide the following identification of tight-binding parameters in terms of circuit elements:

$$
J^\pm = \frac{C_1 \pm C_3}{C_1}, \quad U = \frac{C_U}{C_1}, \quad \varepsilon = \frac{f_0^2}{f^2} - 6, \tag{E3}
$$

where $J^\pm$, U, and ε correspond to the asymmetric hopping strength, the onsite interaction energy, and the eigenenergy of the 1D three-body Bose-Hubbard model. In this case, Eq. (E2) becomes

$$
\varepsilon c_{mnq} = -J^\pm (c_{m\pm1,n,q} + c_{m,n\pm1,q} + c_{m,n,q\pm1})
$$
$$
+ U(\delta_{mn} + \delta_{mq} + \delta_{nq}) c_{mnq}, \tag{E4}
$$

with c_{mnq} corresponding to V_{mnq}. This equation is consistent with the eigenequation of c_{mnq} [Eq. (3) in the main text] for the nonreciprocal 1D Bose-Hubbard model of three bosons. Hence, our designed electric circuits can become an ideal platform for simulating interaction-induced skin effects in the Hilbert space of three bosons.

APPENDIX F: NUMERICAL RESULTS OF CIRCUIT IMPEDANCE RESPONSES

In this appendix, we perform circuit simulations using LTSpice software to illustrate the interaction-induced skin effect in Hilbert space. Here, the values of C_1, C_2, C_U, and L_g are taken as 1 nF, 1 nF, 10 nF, and 3.3 μH. To test
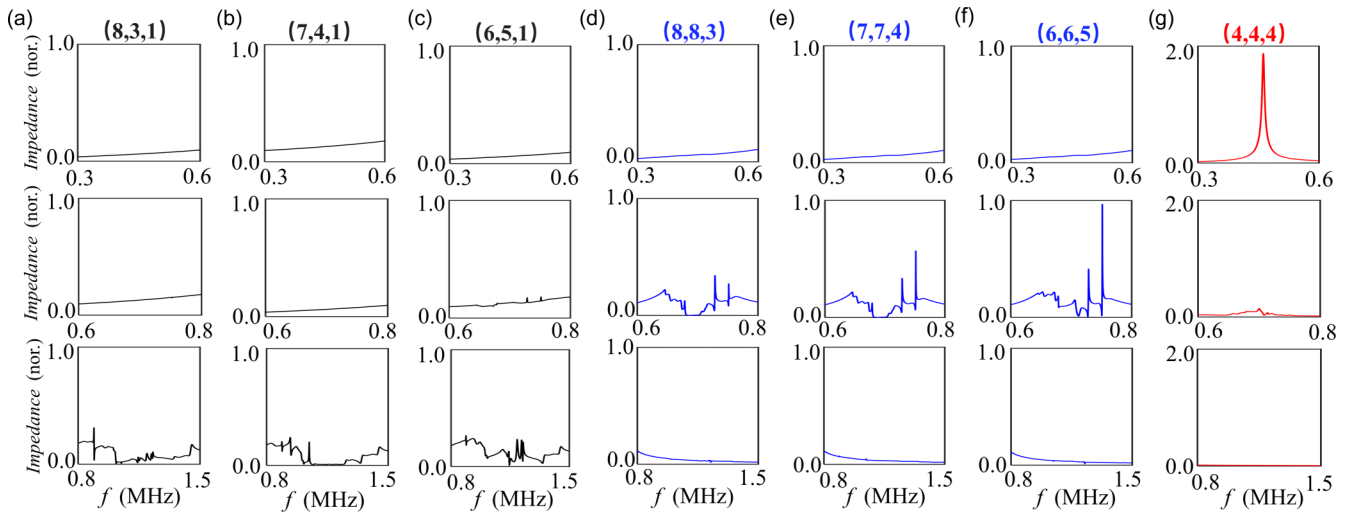
FIG. 9. Numerical results of designed three-dimensional (3D) electric circuits. (a)–(c) The impedance responses of three circuit nodes located in the 3D subspace along $k_{\perp(m,n,q=1)}$. (d)–(f) The impedance responses of three circuit nodes in the two-dimensional (2D) subspace along $k_{\perp(m=n,q)}$. (g) The simulated impedance responses of a circuit node in the one-dimensional (1D) subspace at (4,4,4).

whether skin effects exist in the 3D subspace toward the 2D effective boundary, impedance responses of different circuit nodes along the direction of $\mathbf{k}_{\perp(m=n,q)}$ should be analyzed. Here, we select three circuit nodes in the 3D subspace along $\mathbf{k}_{\perp(m=n,q=1)}$, where the positions of these circuit nodes are labeled by (8,3,1), (7,4,1), and (6,5,1) in Fig. 3(a) of main text. Figures 9(a)–9(c) display numerical results of the calculated impedance (with respect to the ground) of these circuit nodes in three frequency ranges, which correspond to the eigenenergies of three bosons in different subspaces ($\varepsilon \sim 3U$, U, and 0), respectively. It is clearly shown that impedance peaks of the three circuit nodes all appear in the frequency range from 0.8 to 1.5 MHz, matching the corresponding eigenenergy of three bosons in the 3D subspace with $\varepsilon \sim 0$. Moreover, we note that the peak values of these circuit nodes are nearly identical. This indicates that no skin effect appears in the 3D subspace toward the 2D effective boundary, which is in accordance with the theoretical prediction.

Next, the impedance responses of different circuit nodes along the direction of $\mathbf{k}_{\perp(m=n=q)}$ are calculated to prove the existence of skin effects in the 2D subspace toward the 1D effective boundary. Figures 9(d)–9(f) present simulated impedance responses of three selected circuit nodes, which are located at (8,8,3), (7,7,4), and (6,6,5), as marked by blue dots in Fig. 3(a) of the main text. Impedance peaks appear at a frequency of ∼0.69 MHz, which matches the eigenenergy of three bosons in the 2D subspace ($\varepsilon \sim U$). Importantly, it is clearly shown that peak values increase as circuit nodes approach the effective 1D boundary. This phenomenon demonstrates the appearance of skin states in the 2D subspace toward the 1D effective boundary. Finally, the impedance response of a circuit node in the 1D subspace at (4,4,4) is calculated, as shown in Fig. 9(g). We find that good consistency is obtained between the frequency of the impedance peak (∼0.46 MHz) and the three-boson eigenenergy in the 1D subspace ($\varepsilon \sim 3U$).

[1] Y. Nagaoka, Phys. Rev. **147**, 392 (1966).

[2] B. T. Matthias, T. H. Geballe, and V. B. Compton, Rev. Mod. Phys. **35**, 1 (1963).

[3] V. I. Anisimov, J. Zaanen, and O. K. Andersen, Phys. Rev. B **44**, 943 (1991).

[4] D. C. Tsui, H. L. Stormer, and A. C. Gossard, Phys. Rev. Lett. **48**, 1559 (1982).

[5] I. Bloch, J. Dalibard, and W. Zwerger, Rev. Mod. Phys. **80**, 885 (2008).

[6] C. M. Bender and S. Boettcher, Phys. Rev. Lett. **80**, 5243 (1998).

[7] N. Moiseyev, *Non-Hermitian Quantum Mechanics* (Cambridge University Press, Cambridge, 2011).

[8] B. Zhen, C. W. Hsu, Y. Igarashi, L. Lu, I. Kaminer, A. Pick, S.-L. Chua, J. D. Joannopoulos, and M. Soljačić, Nature (London) **525**, 354 (2015).

[9] J. Doppler, A. A. Mailybaev, J. Böhm, U. Kuhl, A. Girschik, F. Libisch, T. J. Milburn, P. Rabl, N. Moiseyev, and S. Rotter, Nature (London) **537**, 76 (2016).

[10] W. Chen, Ş. K. Özdemir, G. Zhao, J. Wiersig, and L. Yang, Nature (London) **548**, 192 (2017).

[11] H. Hodaei, A. U. Hassan, S. Wittek, H. Garcia-Gracia, R. El-Ganainy, D. N. Christodoulides, and M. Khajavikhan, Nature (London) **548**, 187 (2017).

[12] Y.-H. Lai, Y.-K. Lu, M.-G. Suh, Z. Yuan, and K. Vahala, Nature (London) **576**, 65 (2019).

[13] M. P. Hokmabadi, A. Schumer, D. N. Christodoulides, and M. Khajavikhan, Nature (London) **576**, 70 (2019).

[14] Z. Gong, Y. Ashida, K. Kawabata, K. Takasan, S. Higashikawa, and M. Ueda, Phys. Rev. X **8**, 031079 (2018).

[15] V. M. Alvarez, J. B. Vargas, and L. F. Torres, Phys. Rev. B **97**, 121401(R) (2018).

[16] S. Yao and Z. Wang, Phys. Rev. Lett. **121**, 086803 (2018).

[17] C. H. Lee and R. Thomale, Phys. Rev. B **99**, 201103(R) (2019).

[18] D. S. Borgnia, A. J. Kruchkov, and R.-J. Slager, Phys. Rev. Lett. **124**, 056802 (2020).

[19] N. Okuma, K. Kawabata, K. Shiozaki, and M. Sato, Phys. Rev. Lett. **124**, 086801 (2020).

[20] Y. Xiong, J. Phys. Comm. **2**, 035043 (2018).

[21] F. K. Kunst, E. Edvardsson, J. C. Budich, and E. J. Bergholtz, Phys. Rev. Lett. **121**, 026808 (2018).

[22] K. Yokomizo and S. Murakami, Phys. Rev. Lett. **123**, 066404 (2019).

[23] K. Zhang, Z. Yang, and C. Fang, Phys. Rev. Lett. **125**, 126402 (2020).

[24] L. Li, C. H. Lee, S. Mu, and J. Gong, Nat. Commun. **11**, 5491 (2020).

[25] L. Xiao, X. Zhan, Z. H. Bian, K. K. Wang, X. Zhang, X. P. Wang, J. Li, K. Mochizuki, D. Kim, N. Kawakami, W. Yi, H. Obuse, B. C. Sanders, and P. Xue, Nat. Phys. **13**, 1117 (2017).

[26] T. Helbig, T. Hofmann, S. Imhof, M. Abdelghany, T. Kiessling, L. W. Molenkamp, C. H. Lee, A. Szameit, M. Greiter, and R. Thomale, Nat. Phys. **16**, 747 (2020).

[27] A. Ghatak, M. Brandenbourger, J. van Wezel, and C. Coulais, Proc. Natl. Acad. Sci. USA **117**, 29561 (2020).

[28] K. Wang, A. Dutt, K. Y. Yang, C. C. Wojcik, J. Vučković, and S. Fan, Science **371**, 1240 (2021).

[29] J. C. Budich and E. J. Bergholtz, Phys. Rev. Lett. **125**, 180403 (2020).

[30] S. Weidemann, M. Kremer, T. Helbig, T. Hofmann, A. Stegmaier, M. Greiter, R. Thomale, and A. Szameit, Science **368**, 311 (2020).

[31] M. Nakagawa, N. Kawakami, and M. Ueda, Phys. Rev. Lett. **121**, 203001 (2018).

[32] R. Hamazaki, K. Kawabata, and M. Ueda, Phys. Rev. Lett. **123**, 090603 (2019).

[33] K. Yamamoto, M. Nakagawa, K. Adachi, K. Takasan, M. Ueda, and N. Kawakami, Phys. Rev. Lett. **123**, 123601 (2019).

[34] T. Liu, J. J. He, T. Yoshida, Z.-L. Xiang, and F. Nori, Phys. Rev. B **102**, 235151 (2020).

[35] T. Yoshida, K. Kudo, and Y. Hatsugai, Sci. Rep. **9**, 16895 (2019).

[36] D.-W. Zhang, Y.-L. Chen, G.-Q. Zhang, L.-J. Lang, Z. Li, and S.-L. Zhu, Phys. Rev. B **101**, 235150 (2020).

[37] C.-X. Guo, X.-R. Wang, C. Wang, and S.-P. Kou, Phys. Rev. B **101**, 144439 (2020).

[38] S. Mu, C. H. Lee, L. Li, and J. Gong, Phys. Rev. B **102**, 081115(R) (2020).

[39] N. Matsumoto, K. Kawabata, Y. Ashida, S. Furukawa, and M. Ueda, Phys. Rev. Lett. **125**, 260601 (2020).

[40] C. H. Lee, Phys. Rev. B **104**, 195102 (2021).

[41] F. E. Öztürk, T. Lappe, G. Hellmann, J. Schmitt, J. Klaers, F. Vewinger, J. Kroha, and M. Weitz, Science **372**, 88 (2021).

[42] D. O. Krimer and R. Khomeriki, Phys. Rev. A **84**, 041807(R) (2011).

[43] A. Schreiber, A. Gábris, P. P. Rohde, K. Laiho, M. Štefaňák, V. Potoček, C. Hamilton, I. Jex, and C. Silberhorn, Science **336**, 55 (2012).

[44] G. Corrielli, A. Crespi, G. Della Valle, S. Longhi, and R. Osellame, Nat. Commun. **4**, 1555 (2013).

[45] S. Longhi and G. Della Valle, Eur. Phys. J. B **86**, 231 (2013).

[46] N. Hatano and D. R. Nelson, Phys. Rev. Lett. **77**, 570 (1996).

[47] J. Ningyuan, C. Owens, A. Sommer, D. Schuster, and J. Simon, Phys. Rev. X **5**, 021031(R) (2015).

[48] V. V. Albert, L. I. Glazman, and L. Jiang, Phys. Rev. Lett. **114**, 173902 (2015).

[49] C. H. Lee, S. Imhof, C. Berger, F. Bayer, J. Brehm, L. W. Molenkamp, T. Kiessling, and R. Thomale, Commun. Phys. **1**, 39 (2018).

[50] S. Imhof, C. Berger, F. Bayer, J. Brehm, L. W. Molenkamp, T. Kiessling, F. Schindler, C. H. Lee, M. Greiter, T. Neupert, and R. Thomale, Nat. Phys. **14**, 925 (2018).

[51] J. Bao, D. Zou, W. Zhang, W. He, H. Sun, and X. Zhang, Phys. Rev. B **100**, 201406(R) (2019).

[52] W. Zhang, D. Zou, W. He, J. Bao, Q. Pei, H. Sun, and X. Zhang, Phys. Rev. B **102**, 100102(R) (2020).

[53] W. Zhang, D. Zou, Q. Pei, W. He, J. Bao, H. Sun, and X. Zhang, Phys. Rev. Lett. **126**, 146802 (2021).

[54] N. A. Olekhno, E. I. Kretov, A. A. Stepanenko, P. A. Ivanova, V. V. Yaroshenk, E. M. Puhtina, D. S. Filonov, B. Cappello, L. Matekovits, and M. A. Gorlach, Nat. Commun. **11**, 1436 (2020).

[55] W. Zhang, D. Zou, Q. Pei, W. He, H. Sun, and X. Zhang, Phys. Rev. B **104**, L201408 (2021).

[56] D. Zou, T. Chen, W. He, J. Bao, C. H. Lee, H. Sun, and X. Zhang, Nat. Commun. **12**, 7201 (2021).

[57] W. Zhang, H. Yuan, W. He, X. Zheng, N. Sun, F. Di, H. Sun, and X. Zhang, Commun. Phys. **4**, 250 (2021).

[58] W. Zhang, H. Yuan, H. Wang, F. Di, N. Sun, X. Zheng, H. Sun, and X. Zhang, Nat. Commun. **13**, 2392 (2022).

[59] W. Zhang, H. Yuan, N. Sun, H. Sun, and X. Zhang, arXiv:2203.03214.

[60] R. Shen and C. H. Lee, arXiv:2107.03414.